



# Carbon nanotubes/silicon nitride nanocomposites for gasoline lubricated high pressure pumps



C. Pfister<sup>a</sup>, J. Schneider<sup>b</sup>, P. Miranzo<sup>c</sup>, M.I. Osendi<sup>c</sup>, M. Belmonte<sup>c,\*</sup>

<sup>a</sup>Institut fuer Kolbenmaschinen, Karlsruhe Institute of Technology (KIT), Kaiserstrasse 12, 76131 Karlsruhe, Germany

<sup>b</sup>Institute for Applied Materials (IAM-ZBS), Karlsruhe Institute of Technology (KIT), Kaiserstrasse 12, 76131 Karlsruhe, Germany

<sup>c</sup>Institute of Ceramics and Glass (ICV-CSIC), Kelsen 5, 28049 Madrid, Spain

## ARTICLE INFO

### Article history:

Received 2 October 2013

Received in revised form 11 March 2014

Accepted 22 April 2014

Available online 2 May 2014

### Keywords:

A. Ceramic–matrix composites (CMCs)

A. Carbon fibre

B. Wear

D. Mechanical testing

E. Carbon nanotubes

## ABSTRACT

High pressure gasoline direct injection systems are able to considerably reduce both the fuel consumption and the harmful emissions, but the current metallic components should be replaced by new advanced materials with enhanced tribological properties. In this work, multi-walled carbon nanotubes (MWCNTs)/silicon nitride ( $\text{Si}_3\text{N}_4$ ) nanocomposites have been tested in a high-pressure 3-piston prototype pump for gasoline using both a cam/pusher self-mated system, and a nanocomposite cam/steel AISI 52100 pusher configuration.  $\text{Si}_3\text{N}_4$  sliding systems were also tested as reference material. MWCNTs nanocomposite cams in combination with steel pushers present an outstanding performance at high rotation speeds and delivery pressures, showing mechanical efficiencies beyond 0.95, low cyclic variations, and torque oscillations 75% lower than the other tested material combinations. MWCNTs favour the formation of surface dimples where debris are entrapped, and promote tribochemical reactions with the steel pushers, enhancing the mechanical efficiency.

© 2014 Elsevier Ltd. All rights reserved.

## 1. Introduction

The research in gasoline engines is essentially targeted to fuel efficiency, and one of the most promising technologies to attain this goal is the spray-guided direct injection. This technology allows reducing the fuel consumption by up to 50% depending on the engine load and speed [1]. However, injecting the fuel directly into the combustion chamber leads to an increase of the particulate emissions in comparison to conventional gasoline engines [2]. This problem can be significantly overcome augmenting the fuel injection pressure [3,4]. At present, high-pressure gasoline pumps on the market can deliver fuel at maximum pressures of 20 MPa [5,6], but pressure levels up to 80 MPa are required to fully exploit the potential of spray-guided direct injection engines [3,4]. Increasing the pressure level causes considerable tribological stresses to the metallic components within the pump, leading to high friction losses and severe wear particularly due to adhesion. Therefore, under these extreme conditions, the use of advanced materials with enhanced properties, mainly good wear and corrosion resistance as well as low friction coefficient, appears mandatory

for increasing the delivery pressure of high-pressure gasoline pumps.

Non-oxide ceramic materials like silicon carbide (SiC) or silicon nitride ( $\text{Si}_3\text{N}_4$ ) are excellent candidates for this application because of their good thermal, mechanical and tribological properties [7,8]. In fact, preliminary investigations on high-pressure gasoline pumps showed a good performance of SiC at delivery pressures up to 80 MPa [9], while  $\text{Si}_3\text{N}_4$  is already used in combustion engines components and ball bearings [10].

The excellent lubricating properties of graphite are well known [11] and, in this sense, few works have pointed out the lubricating benefits of adding carbon nanostructures (carbon nanotubes or graphene), which present outstanding physical properties [12,13], to a  $\text{Si}_3\text{N}_4$  matrix [14–16]. Actually, some of the present authors have reported that multi-walled carbon nanotubes (MWCNTs) containing  $\text{Si}_3\text{N}_4$  composites extraordinarily enhanced the tribological performance of the monolithics under lubrication with iso-octane, decreasing the friction coefficient and the wear volume in about 40% and 80%, respectively, as compared with the bare  $\text{Si}_3\text{N}_4$  material [14]. Similar trend was evidenced replacing MWCNTs by graphene [16], with a reduction on the friction coefficient of 32% and an increase of 56% on the nanocomposite wear resistance. Under dry testing conditions, Hvizdos et al. [15] observed a negligible influence of MWCNTs on the wear rate of the  $\text{Si}_3\text{N}_4$  materials but the friction coefficient considerably diminished (62%).

\* Corresponding author. Address: Institute of Ceramics and Glass (ICV-CSIC), C/ Kelsen 5, Cantoblanco, 28049 Madrid, Spain. Tel.: +34 917355863; fax: +34 917355843.

E-mail address: [mbelmonte@icv.csic.es](mailto:mbelmonte@icv.csic.es) (M. Belmonte).

The aim of this work is to investigate the potential of MWCNTs/ $\text{Si}_3\text{N}_4$  nanocomposites as sliding components in a gasoline high-pressure prototype pump. Both MWCNTs nanocomposite and reference  $\text{Si}_3\text{N}_4$  were used in a cam/pusher self-mated system and in a ceramic cam/steel AISI 52100 pusher configuration at delivery pressures up to 80 MPa. This pressure level was chosen as a compromise between the advantages of high-pressure injection and the increasing driving power required by the pump [17]. The mechanical efficiency, the torque oscillations, as a measure for the noise emission of the pump, and the worn cam/pusher surfaces were analysed.

## 2. Experimental procedure

### 2.1. Materials

$\text{Si}_3\text{N}_4$  nanocomposites containing 4.6 vol.% of commercial MWCNTs (NC3100, Nanocyl S.A., Belgium) were processed as detailed elsewhere [18]. In brief, an ethanol suspension containing MWCNTs was sonicated in an ultrasonic bath for 1 h, while the  $\text{Si}_3\text{N}_4$  powder composition, consisting of  $\text{Si}_3\text{N}_4$  (SN-E10, UBE Industries, Japan) plus 2 wt.% of  $\text{Al}_2\text{O}_3$  (SM8, Baikowski Chimie, France) and 5 wt.% of  $\text{Y}_2\text{O}_3$  (Grade C, H.C. Starck GmbH & Co., Germany), both used as sintering aids, was attrition milled in ethanol for 2 h employing  $\text{Si}_3\text{N}_4$  balls. Then, both ethanol suspensions were mixed at given proportions in an ultrasonic bath under continuous stirring for an additional 1 h. The resulting MWCNTs/ceramic powder slurry was dried in a rotary evaporator, oven dried at 120 °C for 24 h, and sieved through a 63  $\mu\text{m}$  mesh. A reference  $\text{Si}_3\text{N}_4$  powder composition was also produced for comparison.

Disc specimens of 25 mm  $\times$  3.4 mm (cam) and 20 mm  $\times$  3.4 mm (pusher) were spark plasma sintered (SPS, Dr. Sinter, SPS-510CE, Japan) applying an uniaxial pressure of 50 MPa during the heating cycle, and using a vacuum atmosphere of 4 Pa. The temperatures and the holding times were selected to get fully dense materials with  $\alpha/\beta$ -phase ratio of  $\sim 40/60$ . In this way, a temperature of 1640 °C for 5 and 10 min were selected for nanocomposite pushers and cams, respectively. For the monolithic material, pushers were sintered at 1600 °C for 10 min while temperatures up to 1640 °C for 5 min were required for cams.

Apparent density of the specimens was calculated by water immersion.  $\text{Si}_3\text{N}_4$  crystalline phases and the  $\alpha \rightarrow \beta$  transformation degree were determined by X-ray diffraction (XRD, Bruker D5000, Siemens, Germany) [19]. Micro-Raman spectra of the pristine MWCNTs and the nanocomposites were recorded using a confocal Raman-AFM equipment (Alpha300 WITec GmbH, Germany), and the 532 nm laser excitation wavelength. Fracture surface of the

nanocomposites was observed by scanning electron microscopy (SEM, S-4700, Hitachi).

Elastic modulus ( $E$ ) was measured by the impulse excitation technique. Vickers hardness ( $H_V$ ) and fracture toughness ( $K_{IC}$ ) were determined using an instrumented microindenter (Zwick/Roell, Zhu 2.5) and applying loads of 98 and 196 N, respectively. Bending strength was estimated by three point tests on prismatic bars [20]. At least five measurements were performed per specimen and test.

### 2.2. Prototype pump and test rig

Fig. 1 depicts the main components of the 3-piston prototype pump used for this study. The kinematics can be described as follows: as the eccentric driveshaft rotates, the motion of the cams is described as a circular translation, driving the pistons via the pushers. The piston/pusher assemblies maintain contact with the cams via retaining springs, which are not shown in the figure. The piston/cylinder, cam/pusher and driveshaft/eccentric lobe systems are lubricated by the delivered fuel that flows through the housing before being suctioned in the cylinders (the sealing of the piston/cylinder systems is realized by a throttle gap seal). The joint between the driveshaft and the pump housing is performed by grease lubricated ball bearings. The diameter of the piston is 8 mm and its travel is 4 mm, corresponding to 603  $\text{mm}^3$  pump displacement. The pump is fitted with pressure transducers in each cylinder. The investigations focus on the cam/pusher system because its performance directly affects to the piston/cylinder one, considering that the contact force between the pistons and the cylinders is proportional to the friction force of the corresponding cam/pusher systems.

Two cam/pusher testing configurations were used: self-mated systems and ceramic cam/hardened bearing steel AISI 52100 (Eisen Schmitt, Germany) pusher arrangements. Cams and pushers were glued into metallic holders for easy replacement in the prototype pump (Fig. 2) and fine ground to get an average surface roughness ( $R_a$ ) of 0.1  $\mu\text{m}$  and 0.05  $\mu\text{m}$  for  $\text{Si}_3\text{N}_4$ -based and steel specimens, respectively. In addition, the edges of all specimens were chamfered (0.5 mm, 45°).

The pump was tested under realistic operating conditions. The low rotation speed range of the high-pressure pump, from 300 rpm to 1300 rpm in 200 rpm steps, was investigated since it leads to higher friction losses [9]. The selected rotation speed range corresponded to an average sliding speed between cams and pushers in the prototype pump that varied from 0.040  $\text{ms}^{-1}$  to 0.173  $\text{ms}^{-1}$ . The delivery pressure was changed from 20 MPa to 80 MPa in 10 MPa steps. Every run took about 4 h (220,000 revolutions) and was repeated four times. Unless otherwise mentioned, the data

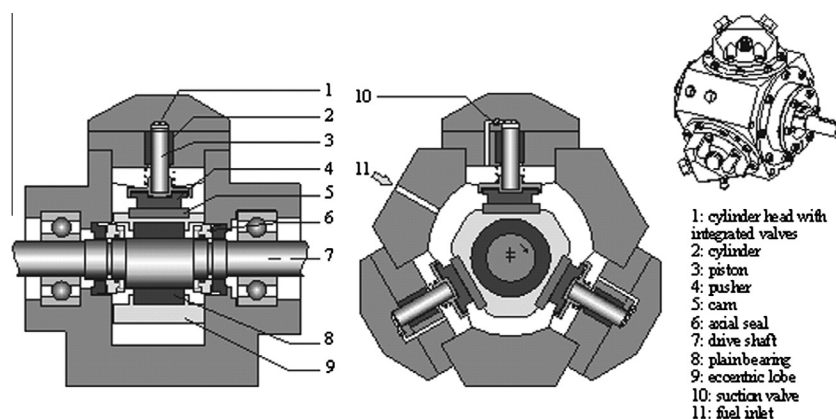


Fig. 1. Schematic view of the investigated prototype pump.

Download English Version:

<https://daneshyari.com/en/article/7213648>

Download Persian Version:

<https://daneshyari.com/article/7213648>

[Daneshyari.com](https://daneshyari.com)